

S & M 0687

# Novel Measuring Method for Detection of Propene Using Zirconia-Based Amperometric Sensor with Oxide-Based Sensing Electrode

Taro Ueda, Vladimir V. Plashnitsa<sup>1</sup>, Perumal Elumalai<sup>1</sup> and Norio Miura<sup>1,\*</sup>

Interdisciplinary Graduate School of Engineering Sciences, Kyushu University,  
Kasuga-shi, Fukuoka 816-8580, Japan

<sup>1</sup>Art, Science and Technology Center for Cooperative Research, Kyushu University,  
Kasuga-shi, Fukuoka 816-8580, Japan

(Received June 27, 2007; accepted August 1, 2007)

**Key words:** gas sensor, propene, amperometric sensor, yttria-stabilized zirconia, ZnO

An amperometric sensor based on yttria-stabilized zirconia (YSZ) and an oxide-based sensing electrode (SE) was examined for the detection of propene. Among the various oxide-based SEs tested, ZnO (+8.5 wt.% Pt) was found to give good sensitivity and selectivity to C<sub>3</sub>H<sub>6</sub> at 600°C. A novel measuring method named “pulsed-potential method” was adopted here to obtain improved sensing characteristics. It was shown that the application of this method to the amperometric sensor resulted in significant enhancement in C<sub>3</sub>H<sub>6</sub> sensitivity. The current response to 400 ppm C<sub>3</sub>H<sub>6</sub> obtained by the “pulsed-potential method” was as high as 95 μA, which is about twenty times higher than that obtained by the conventional “constant-potential method.” It was also found that the C<sub>3</sub>H<sub>6</sub> sensitivity of the sensor was hardly affected by the changes in oxygen and water vapor concentrations in the examined range of 3–20 vol.% and 1–16 vol.%, respectively. Furthermore, the present amperometric sensor exhibited relatively good stability.

## 1. Introduction

In recent years, there has been strong global demand for the detection and *in situ* monitoring of pollutant gases, such as hydrocarbons (HCs), CO and NO<sub>x</sub> that are exhausted from automobiles and various industrial processes. Owing to the large amount of exhaust emission, the automobile industry faces very strict regulations such as Euro 4 and Tire 2. In fact, Euro 4 sets severe upper limit values for HCs, CO and NO<sub>x</sub> in exhausts, which are 0.1, 1.0 and 0.08 g/km, respectively. These limit values should

---

\*Corresponding author: e-mail: miurano@astec.kyushu-u.ac.jp

be reduced further in 2009 (Euro 5 proposal). Such a low limit value is inseparably connected to the development of high-performance sensors which can detect each pollutant gas selectively. Since HCs have strong photochemical reactivity which leads to photochemical smog especially in urban areas, the development of a highly sensitive and selective sensor for HCs is strongly required. As far as the actual application of the sensor in automobile exhausts is concerned, in addition to the high sensitivity and high selectivity to the target gas, the sensor should be operated at high temperature and have an excellent long-term stability as well as an ability to work well even in the presence of water vapor and oxygen in a wide concentration range.

So far, a lot of electrochemical sensors based on solid electrolytes, such as yttria-stabilized zirconia (YSZ) and perovskite-type oxides, have been examined and reported for the detection of toxic gases. Presently, there have been many reports on mixed-potential-type, impedancemetric and amperometric sensors based on these solid electrolytes for the detection of CO,<sup>(1-3)</sup> HCs,<sup>(4-16)</sup> SO<sub>x</sub><sup>(17)</sup> and NO<sub>x</sub>.<sup>(18-32)</sup> However, among the various sensors reported so far, amperometric sensors are considered very attractive owing to their selective detection of HCs and linear dependence of sensitivity to the concentration of the target gas. The main drawbacks of the reported solid-electrolyte amperometric sensors seem to be unsatisfactory sensitivity and stability. These drawbacks limit the development of these amperometric sensors for actual applications. Therefore, improvements of the sensing characteristics of amperometric sensors to HCs are highly required.

In this paper, an amperometric YSZ-based sensor using oxide-based SE was examined to achieve improved sensitivity to C<sub>3</sub>H<sub>6</sub> by adopting a novel measuring method called "pulsed-potential method." In this method, the potential was applied to the SE for a very short duration and the peak current was monitored as a sensing signal. As a result, the C<sub>3</sub>H<sub>6</sub> sensitivity was found to be much improved by the "pulsed-potential method." The detailed sensing characteristics of the present amperometric sensor are described here.

## 2. Materials and Methods

### 2.1 Fabrication of sensor

A commercially available one-end-opened YSZ tube (8 mol% Y<sub>2</sub>O<sub>3</sub>-doped, NKT, Japan) was used for the fabrication of the sensor device. The length of the tube was 300 mm and its inner and outer diameters were 5 and 8 mm, respectively. Each of commercial ZnO, SnO<sub>2</sub>, TiO<sub>2</sub>, Cr<sub>2</sub>O<sub>3</sub>, In<sub>2</sub>O<sub>3</sub> (99.9%, Kishida Chemical, Japan) and NiO (99%, Wako Pure Chemical, Japan) powders together with an appropriate amount of commercial Pt paste (Tanaka Kikinokoku, TR-7601, Japan) was thoroughly mixed with  $\alpha$ -terpineol in the weight ratio of 1:1 and applied as SE on the outer surface of the YSZ tube. In addition, the pure Pt paste was applied on the same surface of the YSZ tube to form a counter electrode (CE) as well as on top of the inner surface of the tube to form a Pt/air reference electrode (RE). Finally, the YSZ tube with these electrodes was sintered at 1200°C for 2 h in air.

## 2.2 Evaluation of sensing characteristics

The fabricated sensor was assembled in a quartz tube and its sensing characteristics were measured using a conventional gas-flow apparatus equipped with a furnace operating at 600°C. The total flow rate of the base gas (dry synthetic air) or the sample gas was fixed at 100 cm<sup>3</sup>/min. The water vapor (1.4–16 vol.% H<sub>2</sub>O) was introduced on the sensor along with the base air or the sample gas using a homemade humidifier. The sample gas containing each of various HCs, as well as NO, NO<sub>2</sub>, CO or H<sub>2</sub>, was prepared by diluting the respective parent gases with dry synthetic air. In the present study, two measuring methods were examined. Figure 1 shows the schematic of the representative current-response curves which can be obtained by both methods. First, the current response of the sensor was measured at a fixed applied potential when the gas flow was changed from the base air to the sample gas. This is the so-called conventional “constant-potential method” (Fig. 1(a)). In contrast, a novel measuring technique named “pulsed-potential method” (Fig. 1(b)) was adopted where the peak current was measured as a sensing signal when the potential was pulsedly applied to the SE under continuous flowing of the sample gas having a fixed concentration. In both cases, the current response was measured using a potentiostat (AUTOLAB®, PGSTAT30, The Netherlands). It is expected that the application of the new “pulsed-potential method” can increase sensitivity to a target gas and also improve the stability of the sensor, owing to the reduction of the current passing through the sensor as well as the time for applying potential.

The current–voltage (polarization) curves in the potential range from 0 to +100 mV (vs. Pt-RE) were measured at 600°C under wet condition at a scan rate of 2 mV/min using a three-electrode configuration in the base gas and the sample gases (200 or 400 ppm) using a potentiostat (Hokuto Denko, HZ-3000, Japan).

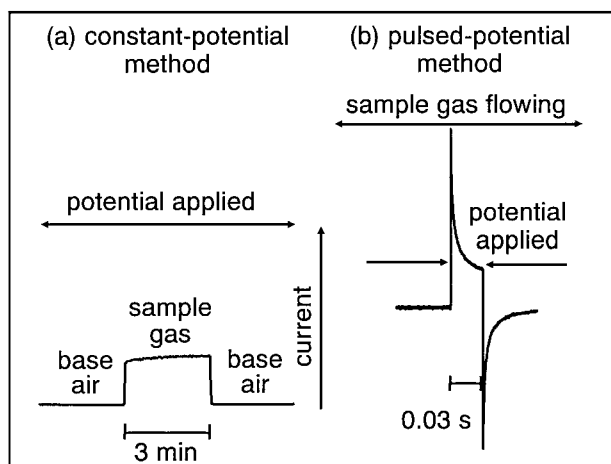


Fig. 1. Schematic views of current response curves for the amperometric sensor: (a) “constant-potential method” and (b) “pulsed-potential method.”

### 2.3 Characterization of sensing material

The microstructure of the SE was observed using a scanning electron microscope (SEM, HITACHI, S-3000N, Japan, operated at 10 kV). The composition analysis of the SE was performed using of an energy dispersive X-ray analyzer (EDX, HORIBA, EX-220SE, Japan). The propene adsorption behavior on the oxide powder (SE) was examined using a Fourier-transform infrared spectrometer (FT-IR, JASCO, DR-600, Japan). A small amount (30 mg) of the oxide powder was put in a cavity-type sample holder. Then, the sample holder was placed in a special chamber attached to a heating facility as well as a provision for gas flowing. The concentration of  $C_3H_6$  was varied from 0 to 800 ppm (in dry synthetic air). The total flow rate of the sample gas was kept at 100  $cm^3/min$ . The FT-IR signal obtained in the base air was taken as background. Then, this background signal was subtracted from that obtained in the sample gas in order to eliminate the influence of the base air on the sample gas signal.

## 3. Results and Discussion

### 3.1 Selection of the best sensing material and operating condition

To select the best sensing material for the detection of HCs, various oxides were examined as SE for the YSZ-based amperometric sensor operated at 600°C under wet condition. The applied potential was kept at +50 mV vs. Pt-RE. Figure 2 shows the comparison of relative sensitivities to  $C_3H_6$  and  $CH_4$  obtained under “constant-potential method” for the amperometric sensors with each of the oxide SEs. The relative sensitivity ( $\Delta I$ )

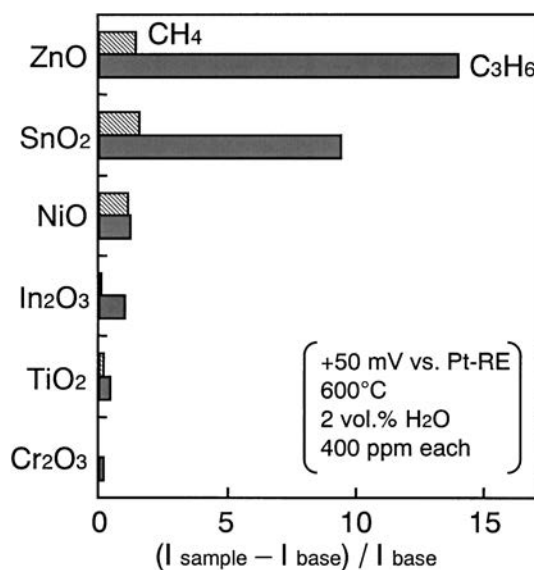


Fig. 2. Comparison of relative sensitivities to  $C_3H_6$  and  $CH_4$  for the sensor with various oxide SEs at 600°C under wet condition (2.0 vol.% H<sub>2</sub>O).

was defined as a ratio  $((I_{\text{sample}} - I_{\text{base}})/I_{\text{base}})$ , where  $I_{\text{sample}}$  is the current response in the sample gas and  $I_{\text{base}}$  is that in the base air. To eliminate the influence of the base current for each oxide SE, the current difference ( $I_{\text{sample}} - I_{\text{base}}$ ) was normalized with the current response obtained in the base air ( $I_{\text{base}}$ ). Among the various oxide SEs tested, ZnO-SE showed the highest sensitivity to  $\text{C}_3\text{H}_6$  with a minor sensitivity to  $\text{CH}_4$  which is usually considered as a nonregulated air pollutant.

The  $\text{C}_3\text{H}_6$  adsorption property of ZnO powder was examined on the basis of *in situ* FT-IR measurements at  $600^\circ\text{C}$ . The obtained results are shown in Fig. 3. It is seen that there are two main peaks at  $1520$  and  $1320\text{ cm}^{-1}$ , corresponding to the stretching vibration of C=C bond and bending vibration of C-H bond, respectively. The intensity of these peaks increased with increasing concentration of  $\text{C}_3\text{H}_6$ . The FT-IR measurement was also carried out using the flow of  $800\text{ ppm CH}_4$  on ZnO powder or  $800\text{ ppm C}_3\text{H}_6$  on NiO powder for comparison, but no peaks were observed in each case. Hence, these results confirm that ZnO in particular can adsorb  $\text{C}_3\text{H}_6$  even at high temperature, and the amount of adsorption increases with increasing concentration of  $\text{C}_3\text{H}_6$ . Thus, the sensor with ZnO-SE seems to exhibit good sensitivity to  $\text{C}_3\text{H}_6$ .

However, the sensor using ZnO-SE showed significant cross-sensitivity to  $\text{NO}_2$ . Thus, to minimize this cross-sensitivity, different amounts of Pt (0–17 wt.%) were added to ZnO-SE as a catalyst for  $\text{NO}_2$  decomposition. As a result, the sensor using ZnO-SE added with 8.5 wt.% Pt (abbreviated as ZnO (+8.5 wt.% Pt)-SE) was found to exhibit almost negligible cross-sensitivity to  $\text{NO}_2$  with a minor change in  $\text{C}_3\text{H}_6$

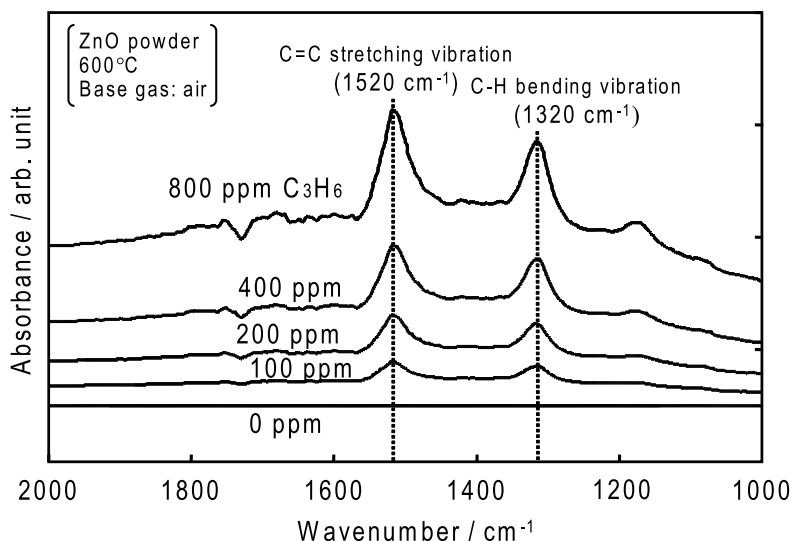


Fig. 3. FT-IR spectra of ZnO powder measured at  $600^\circ\text{C}$  under the flow of  $\text{C}_3\text{H}_6$  (0–800 ppm) diluted with dry air.

response. It seems that the addition of such an amount of Pt is sufficient for the complete decomposition of  $\text{NO}_2$  to  $\text{NO}$ . Figure 4 shows the cross-sectional SEM image (backscattering image) of the YSZ tube with  $\text{ZnO}$  (+8.5 wt.% Pt)-SE. The porous grey layer represents the SE layer with the thickness of about  $35\ \mu\text{m}$ . On the basis of EDX analysis, the bright white dots were confirmed to be Pt particles (mean diameter: *ca.*  $0.8\ \mu\text{m}$ ). It is seen that the Pt particles are dispersed throughout the  $\text{ZnO}$ -SE matrix.

To determine the appropriate applied potential to SE, the polarization curves of the sensor using  $\text{ZnO}$  (+8.5 wt.% Pt)-SE were measured in the base air and in the sample gas containing each of 400 ppm  $\text{C}_3\text{H}_6$ , 400 ppm  $\text{CH}_4$  and 200 ppm  $\text{NO}_2$ , at  $600^\circ\text{C}$  under the wet condition (2 vol.% water vapor). As shown in Fig. 5, the polarization curves in the sample gases containing each of  $\text{NO}_2$  and  $\text{CH}_4$  are not much different from that obtained in the base air. In contrast, the polarization curve in the sample gas containing  $\text{C}_3\text{H}_6$  is considerably different from that in the base air. Thus, it is speculated that only the selective electrochemical reaction involving adsorbed  $\text{C}_3\text{H}_6$  molecules, oxygen ions from the solid electrolyte and electrons from the external circuit, can proceed at the interface between YSZ and  $\text{ZnO}$  (+8.5 wt.% Pt)-SE. On the basis of the results obtained from the polarization curve measurements, the appropriate applied potential to obtain good  $\text{C}_3\text{H}_6$  selectivity for the present sensor can be fixed in the positive potential range above 0 mV vs. Pt-RE. However, to satisfy each of low base current, large current response, quick response/recovery and good stability of current response, the applied potential was fixed hereafter at +70 mV vs. Pt-RE.

### 3.2 Sensing performances of the sensor operated by “constant-potential method”

The sensing characteristics were examined for the sensor with  $\text{ZnO}$  (+8.5 wt.% Pt)-SE operated by the conventional “constant-potential method.” Figure 6 shows the response transients to  $\text{CO}$ ,  $\text{H}_2$ ,  $\text{CH}_4$  and  $\text{C}_3\text{H}_6$  (400 ppm each) as well as to  $\text{NO}$  and  $\text{NO}_2$

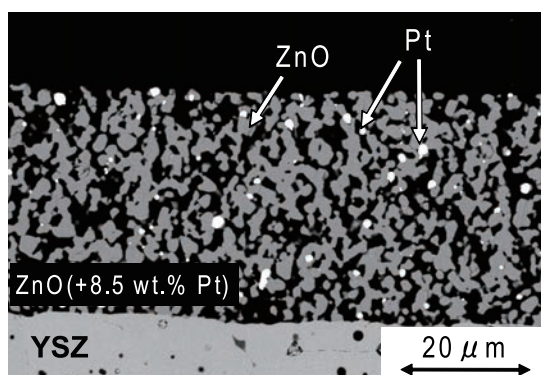


Fig. 4. Cross-sectional SEM image of the YSZ tube with  $\text{ZnO}$  (+8.5 wt.% Pt)-SE sintered at  $1200^\circ\text{C}$ .

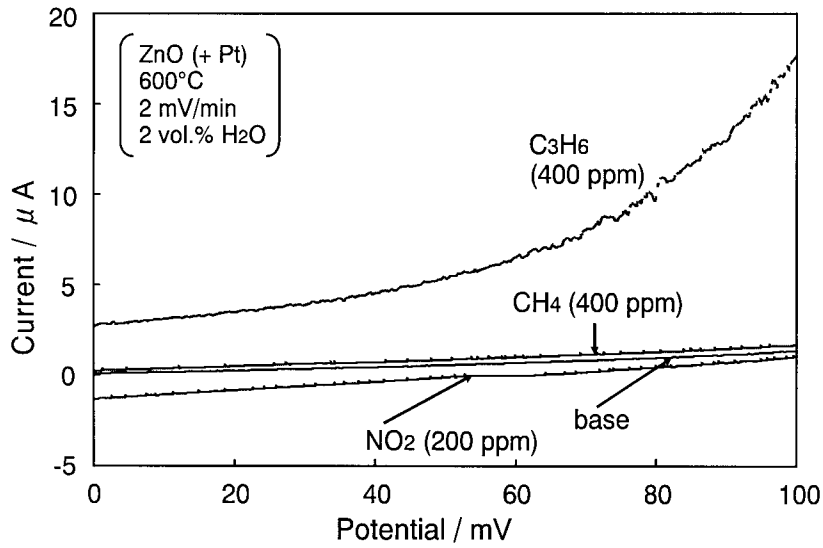


Fig. 5. Polarization curves obtained in the base air and in various sample gases ( $\text{NO}_2$ : 200 ppm,  $\text{CH}_4$ ,  $\text{C}_3\text{H}_6$ : 400 ppm each) in the potential range of 0 – +100 mV (vs Pt-RE) for the sensor with ZnO (+8.5 wt.% Pt)-SE at 600°C under wet condition (2 vol.%  $\text{H}_2\text{O}$ ).

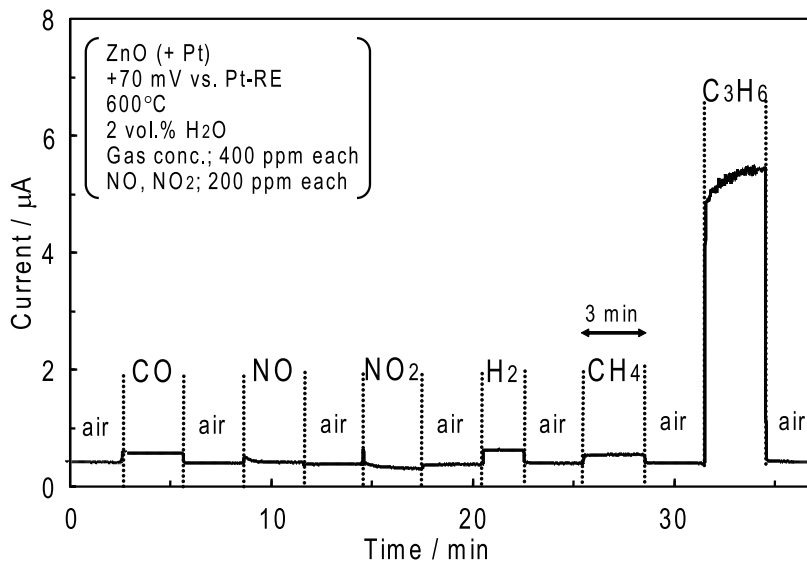


Fig. 6. Response transients to various gases for the sensor with ZnO(+8.5 wt.% Pt)-SE at 600°C under wet condition (2 vol.%  $\text{H}_2\text{O}$ ), applied potential: +70 mV vs Pt-RE.

(200 ppm each) for the present sensor at 600°C under the wet condition. The low base current and the selective response to C<sub>3</sub>H<sub>6</sub> were observed and these results were in good agreement with those obtained from the polarization curve measurements (Fig. 5). The 90% response and 90% recovery rates to 400 ppm C<sub>3</sub>H<sub>6</sub> were found to be less than 10 s. The present sensor also showed a good linear relationship between the sensitivity and the C<sub>3</sub>H<sub>6</sub> concentration in the examined range of 0–800 ppm (not shown here). However, in this case, the obtained sensitivity even to 400 ppm C<sub>3</sub>H<sub>6</sub> was as low as 4 μA, which seems insufficient for a real application.

### 3.3 Sensing performances of the sensor operated by “pulsed-potential method”

To improve the C<sub>3</sub>H<sub>6</sub> sensitivity of the above-mentioned sensor operated under “constant-potential method,” a novel measuring method named “pulsed-potential method” was applied to the same YSZ-based amperometric sensor with ZnO (+8.5 wt.% Pt)-SE. In this “pulsed-potential method,” the potential was pulsedly applied to SE for a short period of 0.03 s under the continuous flow of a certain concentration of sample gas and the peak current was taken as a sensing signal. It is expected that the sensitivity and stability of the sensor can be significantly improved owing to the reduction of total amount of current passed through the sensor. Quite recently, we have reported the preliminary results obtained by this “pulsed-potential method” for the YSZ-based amperometric sensor.<sup>(10)</sup> Here, we examined more detailed sensing characteristics and discussed the difference between the results obtained by both the conventional “constant-potential method” and the new “pulsed-potential method.” For better comparison of the sensing performances, the same applied potential (+70 mV vs. Pt-RE) was used for both cases.

Figure 7 shows the dependence of sensitivity ( $\Delta I$ ) on C<sub>3</sub>H<sub>6</sub> concentration for the sensor operated under both measuring modes. In both cases, the sensitivity varied logarithmically with the C<sub>3</sub>H<sub>6</sub> concentration in the same ranges. Undoubtedly, the C<sub>3</sub>H<sub>6</sub> sensitivity obtained by the “pulsed-potential method” was much higher than that obtained by the “constant-potential method.” For example, the  $\Delta I$  value to 400 ppm C<sub>3</sub>H<sub>6</sub> obtained by the new method is as high as about 95 μA, which is about twenty times higher than that obtained by the conventional method. Figure 8 depicts the cross-sensitivities to various gases (NO, NO<sub>2</sub>: 200 ppm each; CO, H<sub>2</sub>, CH<sub>4</sub>, C<sub>3</sub>H<sub>6</sub>: 400 ppm each) for the sensor with ZnO (+8.5 wt.% Pt)-SE operated at 600°C under the pulsed-potential mode. It is seen that the present sensor gives high sensitivity to C<sub>3</sub>H<sub>6</sub> and quite low cross-sensitivities to the other gases examined, as observed similarly in the case of the “constant-potential method” (Fig. 6).

When the present sensor is considered to be used under an actual exhaust condition, it should work well especially in the wide concentration range of water vapor as well as oxygen without a change in C<sub>3</sub>H<sub>6</sub> sensitivity. Figure 9 shows the dependence of the sensitivity to 100 ppm C<sub>3</sub>H<sub>6</sub> on the concentrations of (a) water vapor (1.4–16 vol.%) and (b) oxygen (3–20 vol.%) for the sensor with ZnO (+8.5 wt.% Pt)-SE at 600°C. It is clear that the C<sub>3</sub>H<sub>6</sub> sensitivity is almost invariant with the change in water vapor concentration in the examined range. Although the C<sub>3</sub>H<sub>6</sub> sensitivity increases slightly with increasing oxygen concentration, the sensitivity deviation is within ±4% in the examined range.



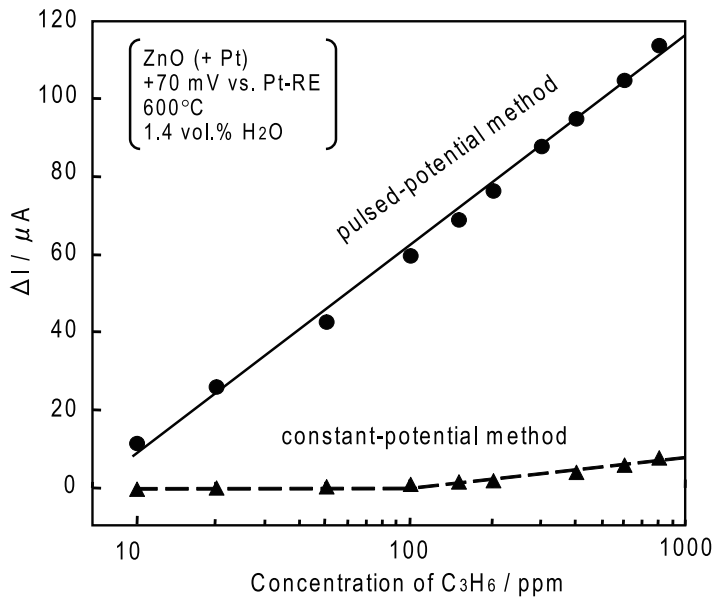


Fig. 7. Dependence of sensitivity on concentration of  $C_3H_6$  at  $600^\circ C$  under wet condition (1.4 vol.%  $H_2O$ ) for the sensor with ZnO (+8.5 wt.% Pt)-SE operated by the “pulsed-potential method” and the “constant-potential method,” applied potential: +70 mV vs Pt-RE.

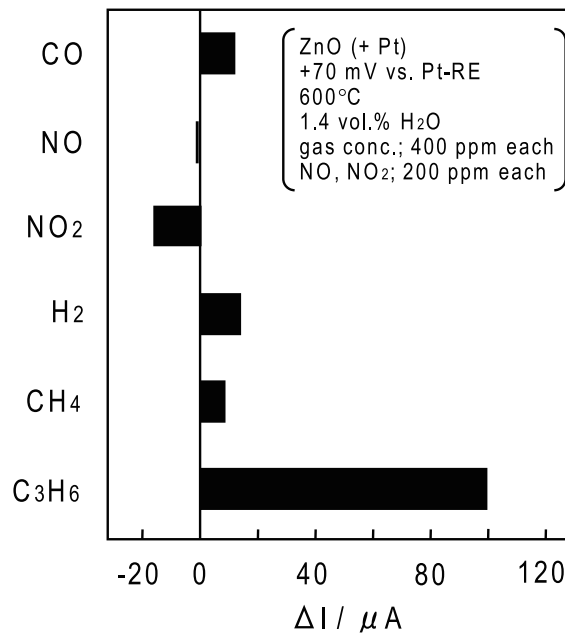


Fig. 8. Cross-sensitivities to various gases at  $600^\circ C$  under wet condition (1.4 vol.%  $H_2O$ ) for the sensor with ZnO (+8.5 wt.% Pt)-SE operated by the “pulsed-potential method,” applied potential: +70 mV vs Pt-RE.

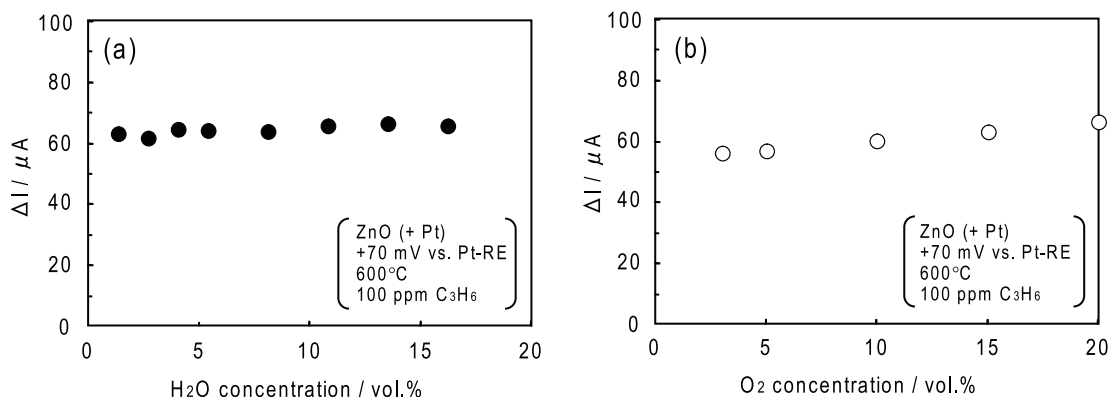


Fig. 9. Dependence of sensitivity to 100 ppm C<sub>3</sub>H<sub>6</sub> on concentrations of (a) oxygen (3–20 vol.%) and (b) H<sub>2</sub>O (1.4–16 vol.%) for the sensor with ZnO (+8.5 wt.% Pt)-SE operated by the “pulsed-potential method” at 600°C, applied potential: +70 mV vs Pt-RE.

Figure 10 shows the comparison of the short-term stability of the sensitivity ( $\Delta I$ ) to 100 ppm C<sub>3</sub>H<sub>6</sub> for the sensor operated under both measuring modes at 600°C under the wet condition. The  $\Delta I$  value was monitored for more than a month. The sensitivity ( $\Delta I_{\text{initial}}$ ) observed on the first measuring day was taken as 100% and the percentage in sensitivity ( $(\Delta I / \Delta I_{\text{initial}}) \times 100$ ) with respect to time was plotted in this figure. In the case of the constant-potential mode, the sensitivity degrades rapidly and goes down to *ca.* 25% of the initial value just after 5 days. Under the pulsed-potential mode, on the other hand, the same amperometric sensor exhibits almost constant sensitivity during the 35 days of testing, although the data were a bit scattered. Such a large improvement in the stability of sensitivity for the sensor operated by the “pulsed-potential method” is attributable to the significant reduction of the total amount of current passing through the sensor as well as the potential application time.

There are various kinds of HCs in exhaust gases emitted from automobiles and industrial processes. Thus, it is also important to examine the cross-sensitivities to various HCs. According to the results reported so far for the solid electrolyte HCs sensors, the sensitivity is usually increased with increasing number of carbon in HCs or degree of unsaturation in C-C bonds.<sup>(5,9,12,16)</sup> Figure 11 shows the cross-sensitivities to various HCs (CH<sub>4</sub>, C<sub>2</sub>H<sub>4</sub>, C<sub>2</sub>H<sub>6</sub>, C<sub>3</sub>H<sub>6</sub>, C<sub>3</sub>H<sub>8</sub>, C<sub>4</sub>H<sub>8</sub>, C<sub>4</sub>H<sub>10</sub>; 100 ppm each) under the wet condition for the sensor with ZnO (+8.5 wt.% Pt)-SE operated by the “pulsed-potential method.” The sensitivity increases with increasing number of carbon in alkanes (or alkenes) as well as C-C unsaturation, as mentioned above.

#### 4. Conclusions

Among the several oxide-SEs tested for the amperometric YSZ-based sensor, ZnO(+8.5 wt.% Pt)-SE gave the highest sensitivity and selectivity at 600°C under wet condition. The C<sub>3</sub>H<sub>6</sub> sensitivity was found to improve by applying the new measuring

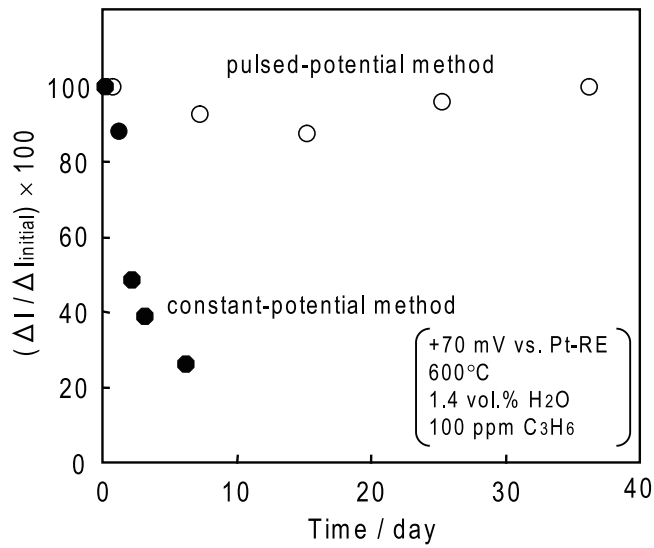


Fig. 10. Time courses of the sensitivity to 100 ppm C<sub>3</sub>H<sub>6</sub> at 600°C under wet condition (1.4 vol.% H<sub>2</sub>O) for the sensor with ZnO (+8.5 wt.% Pt)-SE operated by the “pulsed-potential method” and the “constant-potential method,” applied potential: +70 mV vs Pt-RE.

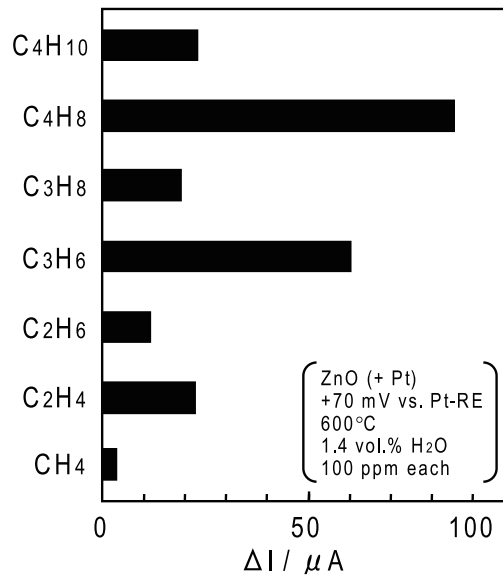


Fig. 11. Cross-sensitivities to various hydrocarbons (100 ppm each) at 600°C under wet condition (1.4 vol.% H<sub>2</sub>O) for the sensors with ZnO (+8.5 wt.% Pt)-SE operated by the “pulsed-potential method,” applied potential: +70 mV vs Pt-RE.

technique, “pulsed-potential method.” The observed sensitivity to  $C_3H_6$  was much higher than that obtained by the conventional “constant-potential method.” The sensor operated under the new measuring mode showed relatively stable behavior throughout the examined period of over a month. The detailed sensing mechanism of this amperometric sensor operated especially under the “pulsed-potential mode” should be investigated for the further improvement in the sensing characteristics.

### Acknowledgements

This work was partially supported through the “Grant-in-Aid for Scientific Research on Priority Area, Nanoionics (439)” by MEXT.

### References

- 1 N. Miura, T. Raisen, G. Lu and N. Yamazoe: *Sens. Actuators B* **47** (1998) 84.
- 2 K. Mochizuki, R. Sorita, H. Takashima, K. Nakamura and G. Lu: *Sens. Actuators B* **77** (2001) 190.
- 3 X. Li and G. M. Kale: *Sens. Actuators B* **123** (2007) 254.
- 4 S. I. Somov and U. Guth: *Sens. Actuators B* **47** (1998) 131.
- 5 T. Hibino and S. Wang: *Sens. Actuators B* **61** (1999) 12.
- 6 T. Ishihara, M. Fukuyama, A. Dutta, K. Kabemura, H. Nishiguchi and Y. Takita: *J. Electrochem. Soc.* **150** (2003) H241.
- 7 A. Dutta, T. Ishihara, H. Nishiguchi and Y. Takita: *J. Electrochem. Soc.* **151** (2004) H122.
- 8 T. Inaba, K. Saji and J. Sakata: *Sens. Actuators B* **108** (2005) 374.
- 9 A. Dutta, H. Nishiguchi, Y. Takita and T. Ishihara: *Sens. Actuators B* **108** (2005) 368.
- 10 T. Ueda, V. V. Plashnitsa, M. Nakatou and N. Miura: *Electrochem. Commun.* **9** (2007) 197.
- 11 N. Miura, T. Shiraishi, K. Shimanoe and N. Yamazoe: *Electrochem. Commun.* **2** (2000) 77.
- 12 A. Hashimoto, T. Hibino, K. Mori and M. Sano: *Sens. Actuators B* **81** (2001) 55.
- 13 R. Mukundan, E. L. Brosha and F. H. Garzon: *J. Electrochem. Soc.* **150** (2003) H279.
- 14 J. Zosel, K. Ahlborn, R. Muller, D. Westphal, V. Vashook and U. Guth: *Solid State Ionics* **169** (2004) 115.
- 15 J. Zosel, R. Müller, V. Vashook and U. Guth: *Solid State Ionics* **175** (2004) 531.
- 16 M. Nakatou and N. Miura: *Sens. Actuators B* **120** (2006) 57.
- 17 Y. Shimizu, M. Okimoto and N. Souda: *Inter J. Appl. Ceram. Technol.* **3** (2006) 193.
- 18 E. D. Bartolomeo, N. Kaabuuathong, M. L. Grilli and E. Traversa: *Solid State Ionics* **171** (2004) 173.
- 19 E. D. Bartolomeo, N. Kaabuuathong, A. D’Epifanio, M. L. Grilli, E. Traversa, H. Aono and Y. Sadaoka: *J. Eur. Ceram. Soc.* **24** (2004) 1187.
- 20 N. Miura, J. Wang, M. Nakatou, P. Elumalai and M. Hasei: *Electrochem. Solid-State Letters* **8** (2005) H9.
- 21 P. Elumalai, J. Wang, S. Zhuiykov, D. Terada, M. Hasei and N. Miura: *J. Electrochem. Soc.* **152** (2005) H95.
- 22 P. Elumalai and N. Miura: *Solid State Ionics* **176** (2005) 2517.
- 23 P. Schmidt-Zhang, W. Zhang, F. Gerlach, K. Ahlborn and U. Guth: *Sens. Actuators B* **108** (2005) 797.
- 24 V. V. Plashnitsa, T. Ueda and N. Miura: *Inter. J. Appl. Ceram. Technol.* **3** (2006) 127.
- 25 E. L. Brosha, R. Mukundan, R. Lujan and F. H. Gargon: *Sens. Actuators B* **119** (2006) 398.

- 26 P. Elumalai, M. Hasei and N. Miura: *Electrochemistry* **2** (2006) 197.
- 27 N. Miura, J. Wang, M. Nakatou, P. Elumalai, S. Zhuiykov and M. Hasei: *Sens. Actuators B* **114** (2006) 903.
- 28 J. Wang, P. Elumalai, D. Terada, M. Hasei and N. Miura: *Solid State Ionics* **177** (2006) 2305.
- 29 M. Nagao, Y. Namekata, T. Hibino, M. Sano and A. Tomita: *Electrochem. Solid-State Letters* **9** (2006) H48.
- 30 A. Dutta and T. Ishihara: *Mater. Manufacturing Processes* **21** (2006) 225.
- 31 P. Elumalai, V. V. Plashnitsa, T. Ueda, M. Hasei and N. Miura: *Ionics* **12** (2007) 331.
- 32 N. Miura, J. Wang, P. Elumalai, T. Ueda, D. Terada and M. Hasei: *J. Electrochem. Soc.* **154** (2007) J246.